Optics Communications 410 (2018) 40–52

Contents lists available at ScienceDirect

Optics Communications

journal homepage: www.elsevier.com/locate/optcom

Influence of microlens array manufacturing errors on light-field imaging

Su-Ning Li, Yuan Yuan *, Bin Liu, Fu-Qiang Wang *, He-Ping Tan

School of Energy Science and Engineering, Harbin Institute of Technology, 92 West Dazhi Street, Harbin 150001, PR China

A R T I C L E I N F O

Keywords:
Light field imaging
Microlens array
Manufacturing error
Image quality evaluation

A B S T R A C T

A microlens array (MLA) is a key optical element for four-dimensional light-field analysis in a light-field camera. MLA manufacturing errors affect light-field imaging, but their effects, especially on the physical imaging process and image-degradation mechanism, have not entirely been studied. In this paper, we develop a manufacturing-error model for MLA and quantitatively analyze raw images and refocused images using image quality evaluation indexes. The results indicate that manufacturing errors cause changes in image features including brightness, resolution, and spot position. The image-features undergo changes and the degree of degradation caused by different error types showed great differences.

1. Introduction

Light-field imaging is a computational imaging technique for capturing and displaying the four-dimensional light-field distribution of a target scene through a single exposure [1]. As compared to the conventional imaging method, which only records two-dimensional position information, light-field imaging technology can simultaneously acquire the position and direction information of spatial light radiation. After processing the light-field data, multi-view imaging, digital refocusing, depth estimation, holographic reconstruction, and other imaging applications can be realized [2]. The light-field camera, also known as plenoptic camera, that is based on a microlens array (MLA), is the most common light-field imaging system. In this camera, the MLA is placed at the focal plane between the main lens and a CCD sensor. Each microlens unit records the scene image from different view angles at a given position by which the light field information from the scene image is acquired [3,4]. Recently, light-field cameras have been widely used in various fields with the development and perfection of light-field imaging theory, algorithm, and camera structure [5–8]. Kim et al. [9] used a light-field camera for human face and iris recognition, and proposed a method for effective defense against face spoofing attacks. Endo et al. [10] developed a computer-generated hologram that achieved 3D reconstruction for real scenes under natural light with a commercial light-field camera Lytro. Apelt et al. [11] observed the morphology of plants and related features in the growth process by using the focus images and depth images provided by a light-field camera. Wang et al. [12] proposed a 3D telemedicine system based on light-field cameras, which can monitor the patient's vital statistics in real time. Wu et al. [13] used a plenoptic camera to eliminate severe image distortion occurring under strong turbulence conditions. Sun et al. [14] introduced a method with a focused light-field camera to reconstruct the three-dimensional temperature field of a flame and experimentally demonstrated the feasibility of the method. Yuan et al. [15] and Huang et al. [16] calculated the temperature distribution and inhomogeneous radiation properties of participating media by using the multispectral light-field imaging technique.

In order to meet the requirements of various applications in different areas, it is necessary to ensure that the target light-field data can be accurately recorded by the light-field camera, which requires the devices to provide high accuracy, and strict registration to be maintained between the devices within the imaging system. However, in the actual design and production process, various errors get inevitably introduced, leading to manufacturing error and coupling misregistration of internal devices, both of which affect the imaging performance. As an optical element to obtain four-dimensional light-field information, the MLA is the key factor in determining the image quality of a light-field camera. Therefore, many researchers have performed studies on the registration error and manufacturing error of MLA. Some studies have made advances in MLA assembly errors for light-field cameras, such as the error model [17], image distortion mechanism [17,18] and error-calibration model [18–20]. In studies concerning manufacturing error, Yang et al. [21] proposed a lens sag detection system using the principle of Fizeau interference, which is applicable to non-contact measurement of spherical MLA with different sizes. You et al. [22] developed a contour error evaluation system that facilitates rational planning of the tool path in MLA processing and improved the MLA

* Corresponding authors.
E-mail addresses: yuanyuan83@hit.edu.cn (Y. Yuan), wangfuqiang@hitwh.edu.cn (F. Wang).

https://doi.org/10.1016/j.optcom.2017.09.055
Received 15 July 2017; Received in revised form 12 September 2017; Accepted 16 September 2017

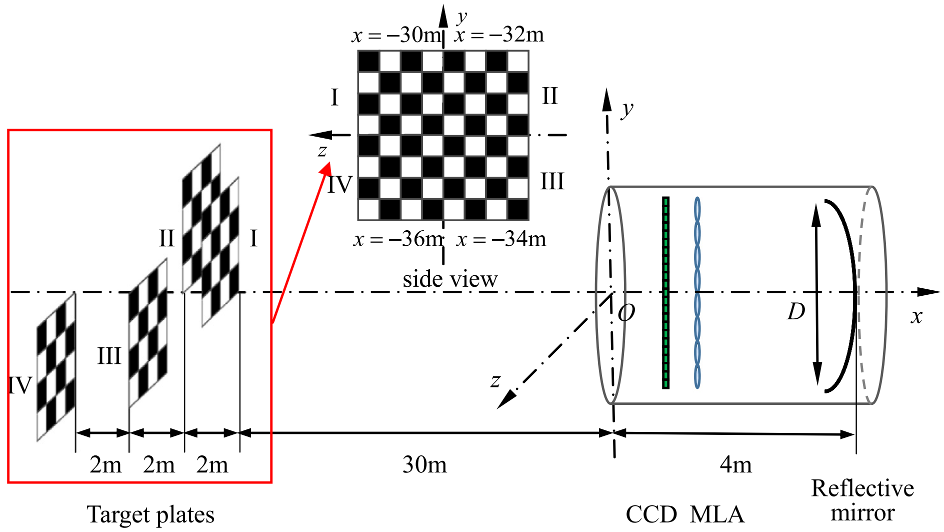

Fig. 1. Structural model of reflective light-field camera.

surface accuracy. Zhong et al. [23] presented an efficient approach to fabricate MLA using polydimethylsiloxane (PDMS). PDMS can be used to prepare larger surface area, concave or convex MLA with arbitrary shape, owing to PDMS properties of easy replica molding and bonding. Liu et al. [24,25] built a fast tool serve (FTS) machining error model for MLA and analyzed the influence of machining errors on form accuracy and uniform optical performance by simulation and experimental methods. Lai et al. [26] adopted a novel micromachining method of electrochemical wet stamping (E-WETS) to fabricate MLA on silicon surface, which is experimentally verified with high accuracy and efficiency, low cost, and easy controllability.

From the above studies, we can see that the current research on MLA manufacturing error has primarily focused on the improvement and optimization of structural design, processing technology and prepared material. The detection of manufacturing errors is largely limited to geometric accuracy evaluation of the MLA surface morphology, and only a few studies have addressed the changes in optical performance (optical parameters such as point spread function and modulation transfer function) of the MLA itself. In fact, it may be difficult to measure the surface shape and optical performance of the overall MLA, where the microlenses are too small in size and large in number. However, there are relatively a few researches on MLA manufacturing error in light-field camera, as compared to the MLA assembly error [17–20]. Further, manufacturing error is also a serious cause of the light-field image quality degradation, and therefore, it is necessary to explore the influence of MLA manufacturing error on the physical imaging process and image-degradation mechanism of the light-field camera imaging system.

Focusing on this problem, in the present study, we construct a manufacturing-error model of MLA, and use a light-field camera imaging simulation system [27] to simulate light-field images under different manufacturing errors. In addition, appropriate image quality evaluation indexes are introduced for quantitatively characterizing the influence of manufacturing errors on imaging. Finally, we analyze the image degradation mechanism caused by manufacturing errors combined with the light-field image and the quality evaluation results. This paper provides the theoretical foundation for the systematic error identification and calibration of light-field camera and the effective detection of MLA machining errors.

2. Model and method

2.1. Light-field camera model

In previous studies, we constructed a simulation model for light-field-camera imaging based on the Monte Carlo method. Related information can be found in reference [27]. In order to simulate the perspective changes and refocusing results more clearly, in this paper we consider a reflecting light-field camera with a large-caliber mirror [17,18,27]. Fig. 1 shows the camera structure model. The camera's main mirror is a reflective mirror with the opening orientation towards the negative direction of the x-axis. The mirror is in the shape of a paraboloid of revolution of diameter $D = 0.8$ m, with its vertex position at $x = 4$ m, and a focal length $f_m = 2.0$ m. The MLA lies on the imaging plane of the reflective mirror, and the CCD sensor is placed at the focal plane of the MLA. The MLA employs a total of 60×60 microlenses. The CCD pixels are of size 0.05 mm, with the pixels on a 600×600 grid. Therefore, each microlens corresponds to 10×10 pixels that record light-field directional information.

To visualize the impact of manufacturing errors on the imaging and focusing performance of the light-field camera, we utilize a set of regular square plates at different depths as the imaging target. The spatial arrangement of plates I, II, III, and IV is shown in Fig. 1, and the distance between adjacent plates is 2 m. Fig. 2 shows the target plate, which is a square of sides 20 cm each that consists of numerous black and white squares of sides 5 cm each. The plate surface is diffuse reflective, where the reflectivity of the white area is 1.0 and that of the black area is 0.0.

2.2. Theoretical model of digital refocusing

The process of light-field refocusing [28] is illustrated by the light-transfer model shown in Fig. 3. In the light-field sampling space, $\boldsymbol{U} = (u, v)$ represents the reflective mirror plane, $\boldsymbol{S} = (s, t)$ represents the sensor plane, and $\boldsymbol{X} = (x, y)$ represents the new focusing plane. F is the separation between the reflective mirror and the sensor, and F' is the new focusing depth from the mirror plane. We define the relative depth of the focusing plane as $\alpha = F'/F$. Let a ray denoted by $L_{F'}$, which travels in a certain direction, intersect the plane $\boldsymbol{U}$ at (u, v) and the plane $\boldsymbol{X}$ at (x, y). As per the geometric construction of Fig. 3, the ray redefined as L_F intersects the plane $\boldsymbol{S}$ at $(s', t') = \left(u + \frac{x-u}{\alpha}, v + \frac{y-v}{\alpha}\right)$.